

Supplemental Data

Supplemental figure legends

Supplemental Fig. S1 Jurkat cells do not express integrin α_M subunit but express chemokine receptor CXCR4. A. Fluorescence intensity histograms of Jurkat cells stained by PE-conjugated anti- α_M mAb or isotype-matched irrelevant IgG in $\text{Ca}^{2+}/\text{Mg}^{2+}$ with or without chemokine CXCL12. B. Fluorescence intensity histograms of polymorphonuclear leukocytes (PMN) stained by PE-conjugated anti- α_M mAb or isotype-matched irrelevant IgG in $\text{Ca}^{2+}/\text{Mg}^{2+}$. C. Fluorescence intensity histograms of Jurkat cells stained by PE-conjugated anti-CXCR4 mAb or isotype-matched irrelevant IgG after incubation with 10 nM CXCL12 for 1 or 2 h in $\text{Ca}^{2+}/\text{Mg}^{2+}$.

Supplemental Fig. S2 Comparison of the three-state (blue solid curves) and two-state (red dashed curves) model fits with the survival frequency (upper row) and rupture probability (lower rows) vs. lifetime data (blue points) measured in $\text{Ca}^{2+}/\text{Mg}^{2+}$ (A), $\text{Ca}^{2+}/\text{Mg}^{2+}/\text{CXCL12}$ (B), $\text{Mg}^{2+}/\text{EGTA}$ (C), Mn^{2+} (D), $\text{Ca}^{2+}/\text{Mg}^{2+}$ plus XVA143 (E), $\text{Ca}^{2+}/\text{Mg}^{2+}/\text{CXCL12}$ plus XVA143 (F), $\text{Mg}^{2+}/\text{EGTA}$ plus XVA143 (G), and Mn^{2+} plus XVA143 (H) for the indicated forces.

Supplemental Fig. S3 Distributions of lifetimes of LFA-1/KIM127 bonds at the indicated forces (the mean \pm s.e.m. of which are shown in Fig. 2C).

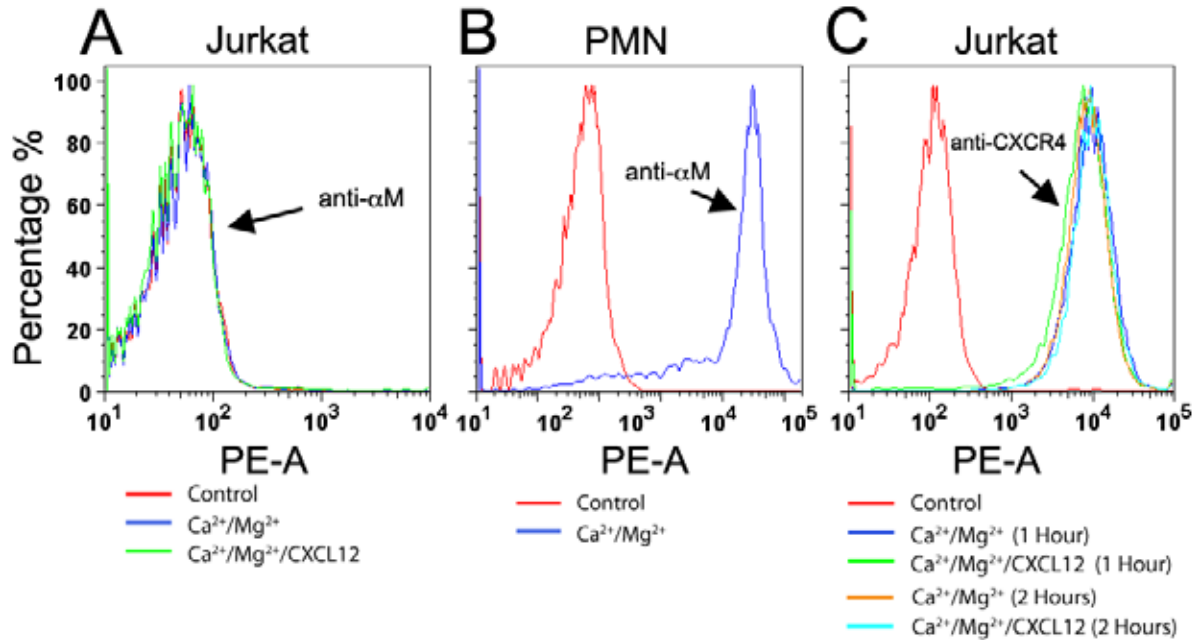
Supplemental Fig. S4 Analysis of lifetimes by a two-state model. Plots of reciprocal off-rates (A-D) or fractions of bonds (B-L) of the short (\square and Δ) and long (\circ and ∇) -lived states estimated from simultaneously fitting the two-state model to the survival frequency (Fig. S2, upper rows) and rupture probability (Fig. S2, lower rows) vs. lifetime data measured in $\text{Ca}^{2+}/\text{Mg}^{2+}$ (A, E, I), $\text{Ca}^{2+}/\text{Mg}^{2+}/\text{CXCL12}$ (B, F, J), $\text{Mg}^{2+}/\text{EGTA}$ (C, G, K) or Mn^{2+} (D, H, L) in the absence (middle row) and presence (bottom row) of XVA143. The off-rates in A-D were required to fit data both in the absence (\square and \circ) and presence (Δ and \diamond) of XVA143.

Supplemental video legends

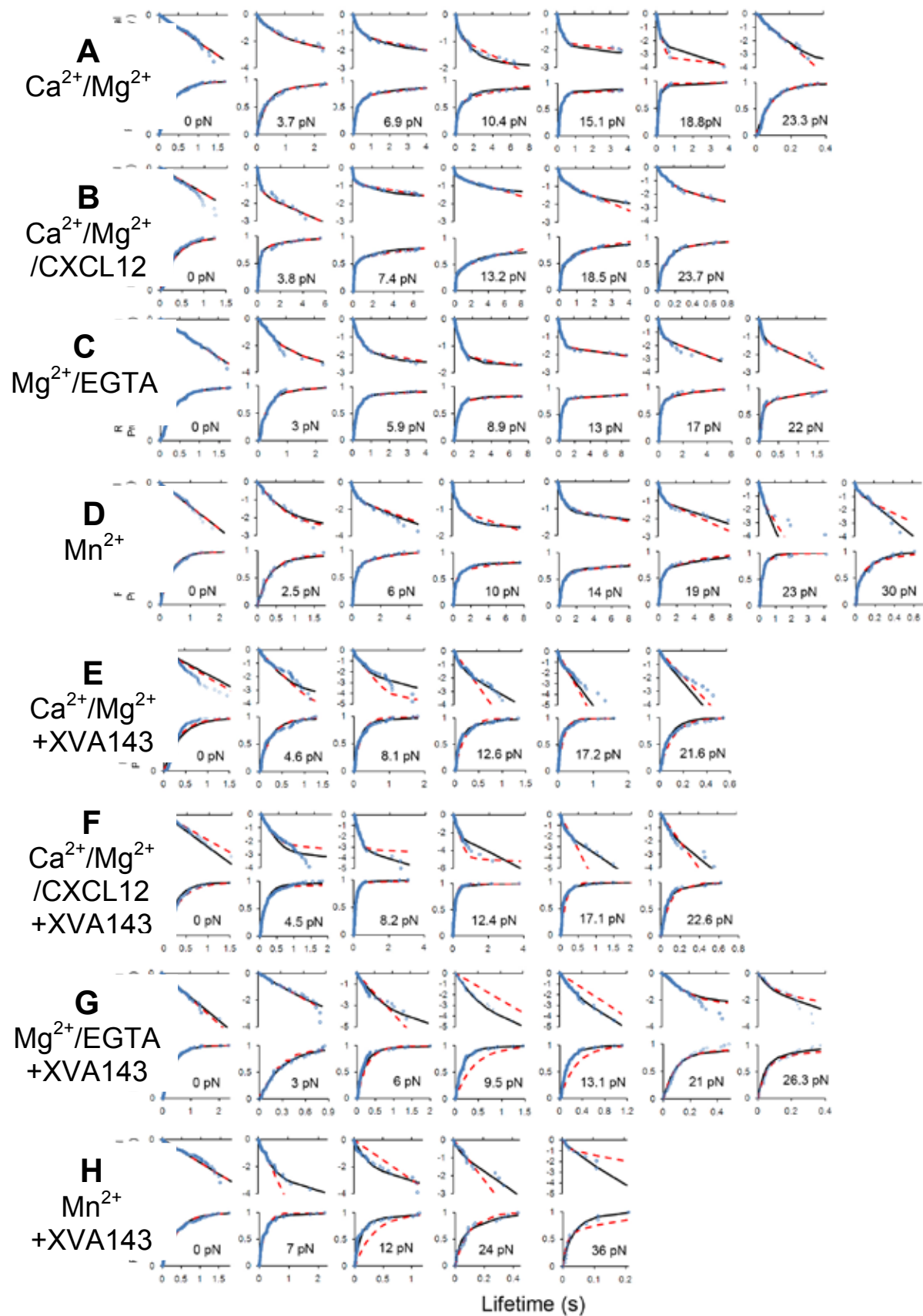
Supplemental video 1 Force-clamp assay for measuring adhesion frequency and bond lifetimes at a constant force. Left panel. Real-time movie of a Jurkat cell (right) driven to contact an ICAM-1-coated bead (attached to the apex of a red blood cell, left) and retract to allow detection of adhesion and to apply a preset force for lifetime measurement. Right panel. Force vs. time data synchronized with the movie.

Supplemental video 2 Thermal fluctuation assay for measuring bond lifetimes at zero force. Left panel. Real-time movie of a Jurkat cell (right) driven to contact an ICAM-1-coated bead (attached to the apex of a red blood cell, left) and retract to the null position for lifetime measurement at zero force. Right panel. BFP position (top) and 70-point sliding standard deviation (bottom) vs. time data synchronized with the movie. Horizontal lines represent thresholds to identify bond association (solid line) and dissociation (dashed line) events, which are marked by the respective down and up arrows.

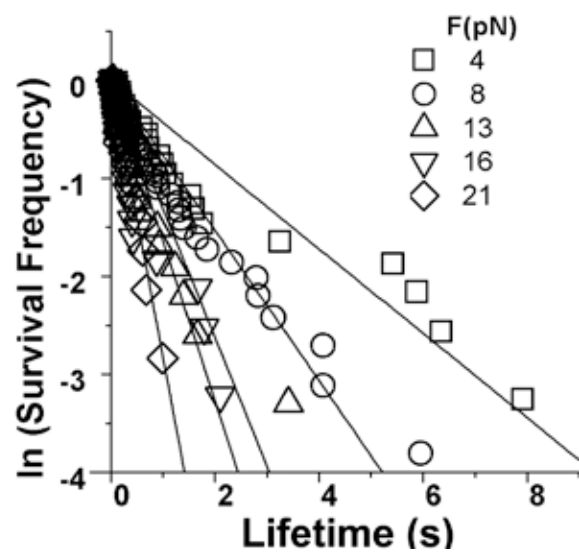
Supplemental figures



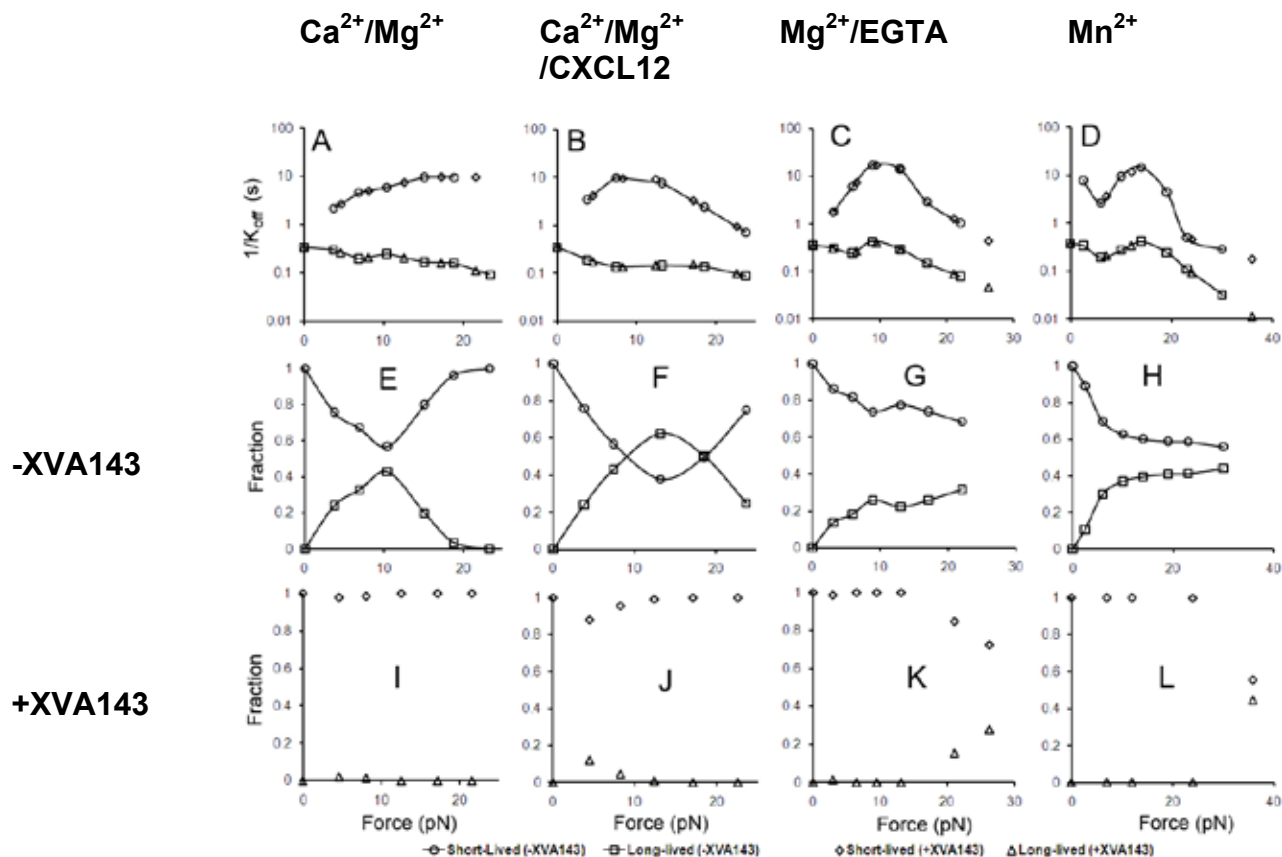
Supplemental Fig. S1 Jurkat cells do not express integrin α_M subunit but express chemokine receptor CXCR4. A. Fluorescence intensity histograms of Jurkat cells stained by PE-conjugated anti- α_M mAb or isotype-matched irrelevant IgG in Ca^{2+}/Mg^{2+} with or without chemokine CXCL12. B. Fluorescence intensity histograms of polymorphonuclear leukocytes (PMN) stained by PE-conjugated anti- α_M mAb or isotype-matched irrelevant IgG in Ca^{2+}/Mg^{2+} . C. Fluorescence intensity histograms of Jurkat cells stained by PE-conjugated anti-CXCR4 mAb or isotype-matched irrelevant IgG after incubation with 10 nM CXCL12 for 1 or 2 h in Ca^{2+}/Mg^{2+} .



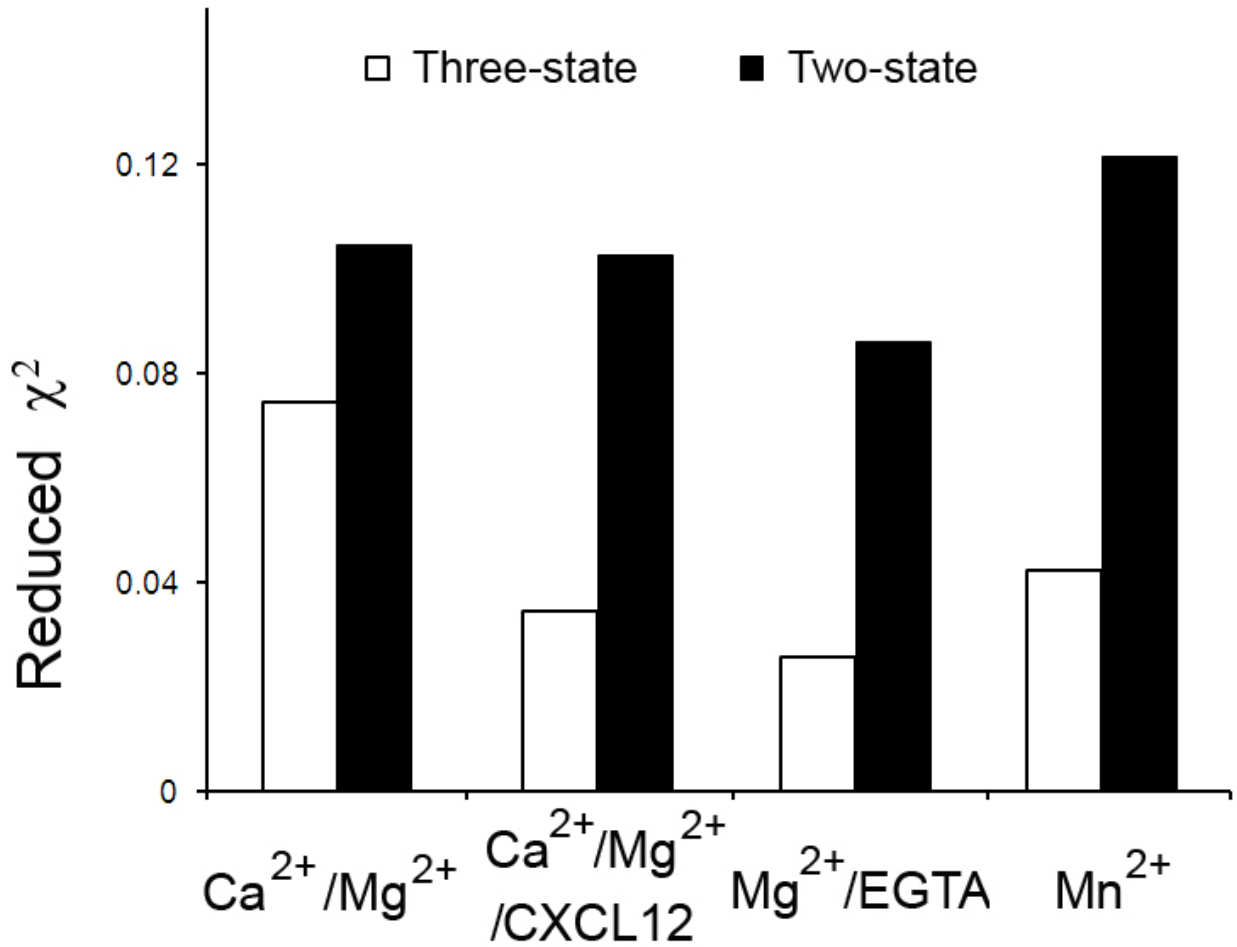
Supplemental Fig. S2 Comparison of the three-state (blue solid curves) and two-state (red dashed curves) model fits with the survival frequency (upper row) and rupture probability (lower rows) vs. lifetime data (blue points) measured in $\text{Ca}^{2+}/\text{Mg}^{2+}$ (A), $\text{Ca}^{2+}/\text{Mg}^{2+}/\text{CXCL12}$ (B), $\text{Mg}^{2+}/\text{EGTA}$ (C), Mn^{2+} (D), $\text{Ca}^{2+}/\text{Mg}^{2+}$ plus XVA143 (E), $\text{Ca}^{2+}/\text{Mg}^{2+}/\text{CXCL12}$ plus XVA143 (F), $\text{Mg}^{2+}/\text{EGTA}$ plus XVA143 (G), and Mn^{2+} plus XVA143 (H) for the indicated forces.



Supplemental Fig. S3 Distributions of lifetimes of LFA-1/KIM127 bonds at the indicated forces (the mean \pm s.e.m. of which are shown in Fig. 2C).



Supplemental Fig. S4 Analysis of lifetimes by a two-state model. Plots of reciprocal off-rates (A-D) or fractions of bonds (B-L) of the short (\square and \triangle) and long (\circ and ∇) -lived states estimated from simultaneously fitting the two-state model to the survival frequency (Fig. S2, upper rows) and rupture probability (Fig. S2, lower rows) vs. lifetime data measured in $\text{Ca}^{2+}/\text{Mg}^{2+}$ (A, E, I), $\text{Ca}^{2+}/\text{Mg}^{2+}/\text{CXCL12}$ (B, F, J), $\text{Mg}^{2+}/\text{EGTA}$ (C, G, K) or Mn^{2+} (D, H, L) in the absence (middle row) and presence (bottom row) of XVA143. The off-rates in A-D were required to fit data both in the absence (\square and \circ) and presence (\triangle and \diamond) of XVA143.



Supplemental Fig. S5 Comparison of reduced chi squares (χ^2) of the three-state (open bars) and two-state (closed bar) model fits in the indicated conditions. F-test shows that the three-state model fits the data significantly better than the two-state model ($p < 0.001$ in all cases)